

# Study on Structural Deflection in Attitude Maneuvers of Flexible Satellite Equipped with Fuel-Efficient Input Shaper

Setyamartana Parman<sup>a,\*</sup>

<sup>a</sup>Department of Mechanical Engineering, Universiti Teknologi PETRONAS, Bandar Seri Iskandar, Perak, Malaysia

\*Corresponding author: setyamartana@petronas.com.my

## Paper History

Received: 16-October-2015

Received in revised form: 27-October-2015

Accepted: 29-October-2015

## ABSTRACT

Input shaping technique can successfully suppresses residual vibration in slew maneuvers of flexible systems. This paper studies transient structural deflections of flexible satellite during attitude maneuvers controlled using input shaper. The satellite consists of a rigid main body and two symmetrical flexible solar panels. The equations of motion of the satellite are derived using Lagrange's formulation, and elastic motions of flexible structures are discretized following the finite element method. The attitude maneuvers are equipped with on-off constant amplitude inputs. For fast maneuver, the satellite has poor accuracy after the maneuver. To resolve this issue, input shaper is applied to maneuver the satellite. Various fuel-efficient shaped inputs are studied in order to conclude the relation of input shape and transient maximum deflection resulted.

**KEY WORDS:** *Fuel-Efficient; Input Shaper; Flexible Satellite; Finite Element; Attitude Maneuver.*

## LIST OF SYMBOLS

$r$	Translational Displacement of Main Body
$d$	Displacement Vector of Flexible Substructures
$\Theta$	Rotational Displacement of Main Body
$\phi$	Roll Angle
$\theta$	Pitch Angle
$\psi$	Yaw Angle

$\omega_0$	Angular Velocity of Satellite Orbit
$m$	Total Mass of Satellite
$I$	Total Inertia Matrix of Satellite
$Q$	Coupling Matrix between Translational and Rotational Motions of Main Body
$W$	Coupling Matrix between Translational Motion of Main Body and Flexible Substructures Displacement
$A$	Coupling Matrix between Rotational Motion of Main Body and Flexible Substructures Displacement
$M$	Mass Matrix of Flexible Substructures
$K$	Stiffness Matrix of Flexible Substructures
$A_i, t_i$	Amplitudes and Time Locations of Input Shaper
$F_b, T_b$	Control Forces and Torques Acting on Main Body
$F_a$	External Forces and Torques Acting on Flexible Substructures
$f$	Number of Degrees of Freedom of Flexible Substructures

## 1.0 INTRODUCTION

A satellite or satellite in operation needs certain accuracies in its attitude. To keep the orientation, the satellite during its operation in space requires frequent corrections of its attitude. Attitude maneuver of rigid satellite can be done without a lot of vibration problems after reaching its desired attitude. For the flexible satellite maneuvering the attitude without regard to system flexibility or without controls on the flexible members, large amplitude transient and steady state oscillations may occur, especially when the system is equipped with on-off jets. Such a system often needs a rest-to-rest attitude maneuver with small vibration both during and at the end of the maneuver. For example, it may be necessary to generate a torque profile such that the satellite is rotated through a desired attitude angle, while the deflections of flexible members remain small throughout the maneuver and go to zero at the end of the maneuver.

To minimize modal vibration in a flexible satellite system, which is equipped with on-off reaction jets, the input shaping methods have been developed [1]. Parman and Koguchi [2-6] demonstrate an application of shaped commands to maneuver attitudes of a flexible satellite with a large number of flexible modes. They show that the resultant vibrations can be reduced drastically when the satellite is subjected to shaped inputs suppressing the vibration at the frequency with largest vibration amplitude. However, the structural deflections of the satellite are still large enough.

To resolve large transient deflection during the maneuver using input shaper, several researchers formulated analytical approximation to be included in the input shaping constraints [7-8]. They used a simple model of two masses connected with a spring and selected a simple configuration of input shape. For this kind of study, the analytical formulation of the input constraints can be easily defined. When the system is having a lot of flexible modes, such as finite element model of flexible satellite, analytical equations in limiting deflections of flexible members become very complicated and impossible to be formulated.

This paper presents computer simulations of attitude maneuvers of a satellite with flexible solar panels equipped with constant-amplitude thrusters. The finite element model of satellite developed by Parman [2, 4-5] is used. The study investigates a condition of the satellite where offset angle of the solar panels is  $30^\circ$ . For this setting angle, there is a coupling motion between roll and yaw displacements of the satellite. The problem appearing in fast maneuver of the satellite under constant-amplitude input is introduced first. Then, fuel-efficient input shapers are applied to overcome the issue. Various results of shaped input are simulated and compared to study the influence of fuelling pulse duration to the solar panel's deflection during transient response.

## 2.0 A SATELLITE WITH SYMMETRICAL FLEXIBLE SOLAR PANELS

The particular satellite investigated in this study is a satellite consisting a main body and two symmetrical solar panels, as shown in Fig. 1. The main body is a rigid cuboid. To identify the satellite attitude relative to an inertial frame  $F_i(O_i X_i Y_i Z_i)$ , a main body fixed frame  $F_b(O_b X_b Y_b Z_b)$  is defined. The solar panels are large and long in sizes and they are supposed as flexible structures. To discretize elastic deformations of the panels, the finite element method (FEM) is used. For this application, each solar panel is divided into 32 rectangular bending plate elements. The elements on the right side are numbered from 1 to 16 and on the left side from 17 to 32, while their nodal points are numbered from 1 to 27 and from 28 to 54. Substructure reference frames  $F_j(O_j X_j Y_j Z_j) (j = 1, 2, \dots, 32)$  are defined to measure displacements of their nodes. The  $Y_j$ -axes ( $j = 1, 2, \dots, 16$ ) of the right side panel are parallel to the  $Y_b$ -axis, while the  $Y_j$ -axes ( $j = 17, 18, \dots, 32$ ) of the left side are anti-parallel. All  $Z_j$ -axes are normal to their panels. The origin of the main body fixed frame  $O_b$  is placed on the mid-point of the longitudinal axis of the solar panels. The solar panels are oriented towards the sun, and the declination with respect to the  $X_b$ -axis is identified by the offset angle  $\delta$ .

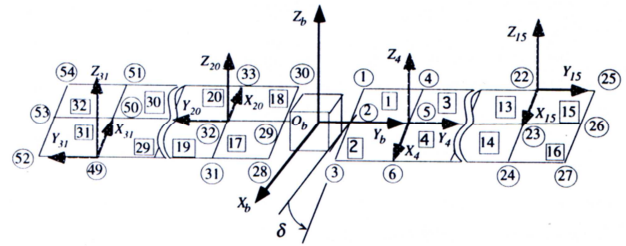


Figure 1: The finite element model of flexible satellite

The attitude angles of the satellite are expressed in Bryant's angles: roll angle  $\phi$ , pitch angle  $\theta$ , and yaw angle  $\psi$ , where the definition of these angles can be seen in Fig. 2. In this figure,  $F_o(X_o Y_o Z_o)$  is the satellite orbital frame.

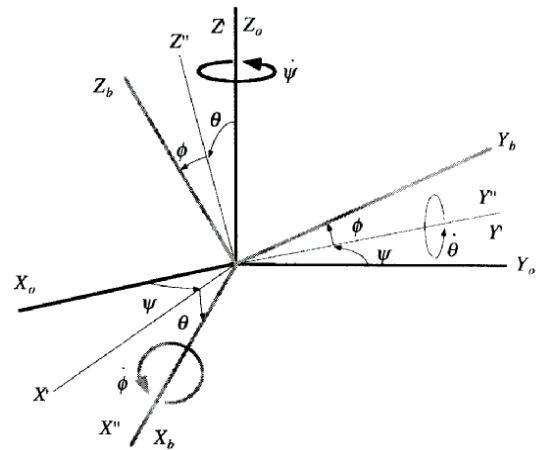


Figure 2: The rotations from observation reference frame  $F_o$  to main body-fixed reference frame  $F_b$

## 2.1 Mathematical Model of Flexible Satellite Dynamics

In this study, equations of motion of general gravity oriented and non-spinning flexible satellite dynamics are derived using a Lagrange's formulation following the works of Parman [2, 4-5]. For this purpose, the expressions of kinetic energy and potential energy for the whole satellite need to be determined first. Since the satellite considered consists of the rigid main body and two flexible solar panels, the kinetic energy and potential energy of the satellite can be formulated by observing the rigid body and flexible solar panels separately. After that, the total satellite kinetic and potential energies can be defined by summing the resulted kinetic and potential energies at above.

### 2.1.1 Kinetic energy.

The kinetic energy of the rigid main body of the satellite can be written in the following form:

$$E_{kb} = \frac{1}{2} \dot{\mathbf{r}}_{i,b}^T \mathbf{r}_{i,b} m_b + \frac{1}{2} \boldsymbol{\omega}_{b,i}^T \mathbf{I}_b \boldsymbol{\omega}_{b,i} + \frac{1}{2} \dot{\mathbf{r}}_{i,b}^T \mathbf{Q}_b \boldsymbol{\omega}_{b,i} \quad (1)$$

where  $\mathbf{r}_{i,b}$  is a vector from  $O_i$  to  $O_b$  (see Fig. 3) with the overdot, ( ) indicating its differentiation with respect to time relative to  $F_i$ ,

$\omega_{b,i}$  is the angular velocity vector of  $F_b$  relative to  $F_i$ ,  $m_b$  is the total mass of the main body,  $\mathbf{I}_b$  is the inertia matrix of the body relative to  $O_b$ , and  $\mathbf{Q}_b$  is the coupling matrix between translational and rotational displacements of the main body. If  $O_b$  coincides with the center of mass of the main body, the value of  $\mathbf{Q}_b$  equals zero.

The kinetic energy of flexible solar panels can be written in the following form:

$$E_{ka} = \frac{1}{2} \dot{\mathbf{r}}_{i,b}^T \dot{\mathbf{r}}_{i,b} m_a + \frac{1}{2} \dot{\mathbf{d}}^T \mathbf{M} \dot{\mathbf{d}} + \frac{1}{2} \omega_{b,i}^T \mathbf{I}_a \omega_{b,i} + \omega_{b,i}^T \mathbf{A} \dot{\mathbf{d}} + \dot{\mathbf{r}}_{i,b}^T \mathbf{W} \dot{\mathbf{d}} + \dot{\mathbf{r}}_{i,b}^T \mathbf{Q}_a \omega_{b,i} \quad (2)$$

where  $\mathbf{d}$  is the displacement vector of flexible solar panels,  $m_a$  is the mass of solar panels,  $\mathbf{M} = \sum_{j=1}^N \mathbf{P}_j^T \mathbf{M}_j \mathbf{P}_j$  is their mass matrix, and  $\mathbf{I}_a = \sum_{j=1}^N \mathbf{T}_j^T \mathbf{I}_j \mathbf{T}_j$  is their inertia matrix with respect to  $O_b$ . The coupling matrices  $\mathbf{A} = \sum_{j=1}^N \mathbf{T}_j^T \mathbf{A}_j \mathbf{P}_j$  and  $\mathbf{W} = \sum_{j=1}^N \mathbf{T}_j^T \mathbf{W}_j \mathbf{P}_j$  relate the main body rotational and translational displacements, respectively, to the solar panel displacements, while  $\mathbf{Q} = \sum_{j=1}^N \mathbf{T}_j^T \mathbf{Q}_j \mathbf{T}_j$  is the coupling matrix between the translational and rotational displacements of the main body contributed by the undeform-state solar panels. In these matrices,  $N$  is the number of elements of flexible solar. For the  $j$ th element,  $\mathbf{T}_j$  is the transformation matrix from  $F_b$  to  $F_j$ ,  $\mathbf{P}_j$  is the assembling matrix relating the element displacement vector  $\mathbf{d}_j$  and the displacement vector of flexible solar panels  $\mathbf{d}$  in the form of  $\mathbf{d}_j = \mathbf{P}_j \mathbf{d}$ ,  $\mathbf{M}_j = \int_{m_j} \mathbf{C}_j^T \mathbf{C}_j dm$  is the mass matrix,  $\mathbf{A}_j = \int_{m_j} {}^j \tilde{\mathbf{r}}_{b,o} \mathbf{W}_j + \int_{m_j} {}^j \tilde{\mathbf{r}}_{o,p_0} \mathbf{C}_j dm$  are the coupling matrices between rotational and translational displacements of the main body respectively and the element displacements,  $\mathbf{Q}_j = \int_{m_j} ({}^j \tilde{\mathbf{r}}_{b,o} + {}^j \tilde{\mathbf{r}}_{o,p_0})^T dm$  is the coupling matrix for the translational and rotational displacements of the main body contributed by the undeform-state element, and  $\mathbf{I}_j = \int_{m_j} ({}^j \tilde{\mathbf{r}}_{b,o} + {}^j \tilde{\mathbf{r}}_{o,p_0})^T ({}^j \tilde{\mathbf{r}}_{b,o} + {}^j \tilde{\mathbf{r}}_{o,p_0}) dm$  is the element inertia matrix with respect to  $O_b$ .  $\mathbf{C}_j$  is the element shape function matrix,  ${}^j \tilde{\mathbf{r}}_{b,o}$  and  ${}^j \tilde{\mathbf{r}}_{o,p_0}$  are vectors from  $O_b$  to  $O_j$  and from  $O_j$  to a particle  $p$  with mass  $dm$  of the element in the undeform state respectively expressed in  $F_j$ , while a general notation of  $(\tilde{\quad})$  means the skew symmetric matrix of a prescribed vector.

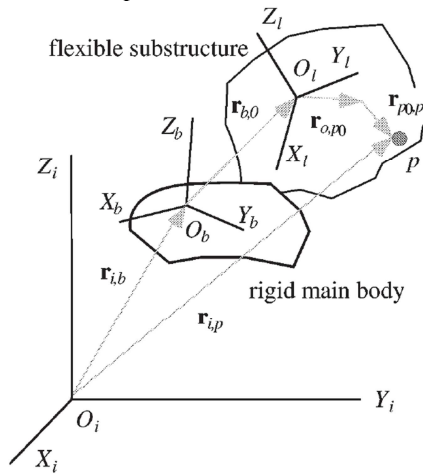


Figure 3: Position vectors from  $F_i(X_iY_iZ_i)$  to a particle  $p$

### 2.1.2 Potential Energy

The potential energy of the satellite consists of the potential energy of its undeform state and the potential energy due to elastic deformations of flexible solar panels. The potential energy of the undeform state, in this study, is measured relative to the earth. When the satellite orbit is circular, it can be expressed as

$$E_{pr} = E_{pr}(\mathbf{r}_{i,b}) \quad (3)$$

The potential energy due to elastic deformations is the sum of the strain energy of flexible substructures and the potential energy due to external forces acting on the substructures with a minus sign. By following the general finite element method procedures, the potential energy due to the elastic deformations of flexible solar panels can be written in the following form:

$$E_{pa} = \frac{1}{2} \mathbf{d}^T \mathbf{K} \mathbf{d} + \mathbf{d}^T \mathbf{F}_a \quad (4)$$

where  $\mathbf{K} = \sum_{j=1}^N \mathbf{P}_j^T \mathbf{K}_j \mathbf{P}_j$  is the stiffness matrix of the solar panels and  $\mathbf{F}_a = \sum_{j=1}^N \mathbf{P}_j^T \mathbf{f}_j$  is the discrete external forces vector acting on the solar panels. For the  $j$ th element,  $\mathbf{f}_j = \int_{V_j} \mathbf{C}_j^T \mathbf{F}_f dV$  is the discrete external forces vector acting on the nodes and  $\mathbf{K}_j = \int_{V_j} \mathbf{C}_j^T \mathbf{B}_j^T \mathbf{R}_j \mathbf{B}_j \mathbf{C}_j dV$  is the stiffness matrix.  $\mathbf{F}_f$  is a distributed external forces vector working on the element,  $\mathbf{B}_j$  is an operator matrix containing first or second order derivative operators, and  $\mathbf{R}_j$  is an elasticity matrix of element  $j$ .

### 2.1.3 Full model equations of motion of flexible satellite

To derive the equations of motion by following Lagrangian procedure, the Lagrangian operator,  $L = E_k - E_p$ , and Lagrange's equations of motion,  $\frac{d}{dt} \left( \frac{\partial L}{\partial \dot{\mathbf{q}}} \right) - \frac{\partial L}{\partial \mathbf{q}} + \frac{\partial S}{\partial \mathbf{q}} = \mathbf{F}$  are used. In these expressions,  $E_k = E_{ka} + E_{kb}$  is the satellite total kinetic energy,  $E_p = E_{pa} + E_{pr}$  is the satellite total potential energy,  $\mathbf{q}$  is the satellite general displacement vector,  $\mathbf{F}$  is the general external forces vector working on the satellite,  $S = \frac{1}{2} \dot{\mathbf{q}}^T \mathbf{D} \dot{\mathbf{q}}$  is the satellite Rayleigh's dissipation, where  $\mathbf{D}$  is the satellite damping matrix. Then, it is considered that control (external) forces acting on the rigid main body of the satellite are much larger than the forces resulting from the potential energy of the undeform state. For simplicity,  $\omega_{b,i}$  and  $\mathbf{r}_{i,b}$  then will be written as  $\omega$  and  $\mathbf{r}$  only, respectively, in this paper.

By using Eqs. (1)-(4), the equations of motion of the satellite can then be linearized and written as follows:

$$\begin{bmatrix} m\mathbf{U}_3 & \mathbf{Q} & \mathbf{W} \\ \mathbf{Q}^T & \mathbf{I} & \mathbf{A} \\ \mathbf{W}^T & \mathbf{A}^T & \mathbf{M} \end{bmatrix} \begin{bmatrix} \dot{\mathbf{r}} \\ \dot{\tilde{\boldsymbol{\omega}}} \\ \dot{\mathbf{d}} \end{bmatrix} + \begin{bmatrix} \mathbf{0}_{3 \times 3} & \mathbf{Q} \tilde{\boldsymbol{\omega}}_0 & \mathbf{0}_{3 \times f} \\ \mathbf{0}_{3 \times 3} & \mathbf{I} \tilde{\boldsymbol{\omega}}_0 & \mathbf{0}_{3 \times f} \\ \mathbf{0}_{f \times 3} & \mathbf{A}^T \tilde{\boldsymbol{\omega}}_0 & \mathbf{D} \end{bmatrix} \begin{bmatrix} \mathbf{r} \\ \tilde{\boldsymbol{\omega}} \\ \mathbf{d} \end{bmatrix} + \begin{bmatrix} \mathbf{0}_3 \\ \mathbf{0}_3 \\ \mathbf{K} \mathbf{d} \end{bmatrix} = \begin{bmatrix} \mathbf{F}_b \\ \mathbf{T}_b \\ \mathbf{F}_a \end{bmatrix} \quad (5)$$

In Eq. (5),  $m$  is the total mass of the satellite,  $\mathbf{Q}$  is the total coupling matrix for the translational and rotational displacements of the rigid main body,  $\mathbf{W}$  is the total coupling matrix for the translational displacements of the rigid main body and the displacements of flexible solar panels,  $\mathbf{I}$  is the total inertia matrix,  $\mathbf{A}$  is the total coupling matrix for the rotational displacements of the rigid main body and the displacements of flexible solar panels. The  $\mathbf{M}$ ,  $\mathbf{D}$  and  $\mathbf{K}$  are the mass, damping and stiffness matrices of the flexible solar panels, respectively. The  $\tilde{\boldsymbol{\omega}}_0$  is the skew symmetric matrix of angular velocity of the satellite orbit

$\mathbf{w}_0$ ,  $\mathbf{r}$  is the translational displacement of the rigid main body,  $\Theta$  is the rotational displacement of the rigid main body which is expressed in a vector of Bryant's angles, and  $\mathbf{d}$  is the displacements of the flexible solar panels.  $\mathbf{F}_b$  and  $\mathbf{T}_b$  are external forces and torques vectors acting on the rigid main body,  $\mathbf{F}_a$  is the vector of external forces and torques acting on the solar panels, while  $f$  is the total number of degrees of freedom of the solar panels. In this paper, the flexible structural subsystems are supposed to have no dissipation properties, so that  $\mathbf{D} = \mathbf{0}$ .

## 2.2 Solar Panels as a Collection of Rectangular Plate Elements

The equations of motion of general satellite have been formed in Eq. (5). To use this equation, the mass and stiffness matrices need to be evaluated for a particular flexible substructure discretization. In this paper, the attitude of the hypothetical satellite is chosen as follows: the  $Z_b$ -axis should point to the centre of earth, the  $Y_b$ -axis is normal to the orbital plane, and the  $X_b$ -axis should point to the satellite linear velocity when there are no attitude errors. For the application of finite element method to discretize elastic deformations of solar panels, the following idealizations are used:

- The solar panels are divided into rectangular flat plate bending elements.
- Each element has a uniform mass density.
- Only out-of-plane deformations of solar panels are considered.
- External loads (both forces and torques) on the solar panels are assumed to work on the nodal points of the elements.
- The  $Y_r$ -axes of elements and the  $Y_b$ -axis of main body frame are parallel or antiparallel (see Fig. 1). The  $X_r$ -axes and  $Y_r$ -axes of elements are in the panel plane, and their  $Z_r$ -axes are normal to the plane.

By using the above idealizations, each element of solar panel has 12 degrees of freedom in total, as shown by Fig. 4. Also, the material of solar panels are assumed as isotropic materials. For an isotropic plate,  $\mathbf{R}_j$  can be written as

$$\mathbf{R}_j = \frac{Ec^3}{12(1-\nu^2)} \begin{bmatrix} 1 & \nu & 0 \\ \nu & 1 & 0 \\ 0 & 0 & \frac{1-\nu}{2} \end{bmatrix} \quad (6)$$

where  $E$ ,  $c$  and  $\nu$  are the Young's modulus, thickness, and Poisson's ratio of  $j$ -th element, respectively.

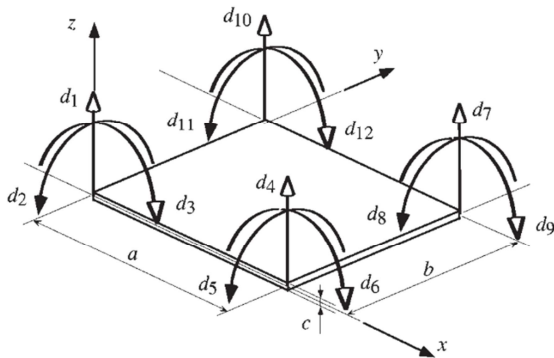


Figure 4: A rectangular plate element model of solar panel with out-of-plane displacement.

The shape function matrix introduced by Bogner [9] is selected. This shape function matrix can guarantee that deflections and slopes are all continuous on the edge of the element, and its expression for the  $j$ -th element is as follows:

$$\mathbf{C}_j^T = \begin{bmatrix} (1+2\xi)(1-\xi)^2(1+2\eta)(1-\eta)^2 \\ (1+2\xi)(1-\xi)^2\eta(1-\eta)^2b \\ -\xi(1-\xi)^2(1+2\eta)(1-\eta)^2a \\ (1+2\xi)(1-\xi)^2(3-2\eta)\eta^2 \\ -(1+2\xi)(1-\xi)^2(1-\eta)\eta^2b \\ -\xi(1-\xi)^2(3-2\eta)\eta^2a \\ (3-2\xi)\xi^2(3-2\eta)\eta^2 \\ -(3-2\xi)\xi^2(1-\eta)\eta^2b \\ (1-\xi)\xi^2(3-2\eta)\eta^2a \\ (3-2\xi)\xi^2(1+2\eta)(1-\eta)^2 \\ (3-2\xi)\xi^2\eta(1-\eta)^2b \\ (1-\xi)\xi^2(1+2\eta)(1-\eta)^2a \end{bmatrix} \quad (7)$$

where  $a$  and  $b$  are the length and width of element, respectively,  $0 \leq (\xi = x/a) \leq 1$ , and  $0 \leq (\eta = y/b) \leq 1$ . For this shape function matrix, the coupling matrix  $\mathbf{A}_j$  can be obtained as follows:

$$\mathbf{A}_j^T = \frac{\rho abc}{24} \begin{bmatrix} 6y_{0j} + \frac{9}{5}b & -6x_{0j} - \frac{9}{5}a & 0 \\ by_{0j} + \frac{2}{5}b^2 & -bx_{0j} - \frac{3}{10}ab & 0 \\ -ay_{0j} - \frac{3}{10}ab & ax_{0j} + \frac{2}{5}a^2 & 0 \\ 6y_{0j} + \frac{21}{5}b & -6x_{0j} - \frac{9}{5}a & 0 \\ -by_{0j} - \frac{3}{5}b^2 & bx_{0j} + \frac{3}{10}ab & 0 \\ -ay_{0j} - \frac{7}{10}ab & ax_{0j} + \frac{2}{5}a^2 & 0 \\ 6y_{0j} + \frac{21}{5}b & -6x_{0j} - \frac{21}{5}a & 0 \\ -by_{0j} - \frac{3}{5}b^2 & bx_{0j} + \frac{7}{10}ab & 0 \\ ay_{0j} + \frac{7}{10}ab & -ax_{0j} - \frac{3}{5}a^2 & 0 \\ 6y_{0j} + \frac{9}{5}b & -6x_{0j} - \frac{21}{5}a & 0 \\ by_{0j} + \frac{2}{5}b^2 & -bx_{0j} - \frac{7}{10}ab & 0 \\ ay_{0j} + \frac{3}{10}ab & -ax_{0j} - \frac{3}{5}a^2 & 0 \end{bmatrix} \quad (8)$$

where  $x_{0j}$  and  $y_{0j}$  are the components of  ${}^l\mathbf{r}_{b,o}$  for the  $j$ -th element along its  $X_r$  and  $Y_r$ -axes, respectively (see Figs. 1 and 3),  $\rho$  is the mass density, while the inertia matrix  $\mathbf{I}_j$  can be written as follows:

$$\mathbf{I}_j = \rho abc \begin{bmatrix} I_{j11} & I_{j21} & I_{j31} \\ I_{j21} & I_{j22} & I_{j32} \\ I_{j31} & I_{j32} & I_{j33} \end{bmatrix} \quad (9)$$

where

$$\begin{aligned} I_{j11} &= y_{0j}^2 + \frac{1}{12}c^2 + \frac{1}{3}b^2 + y_{0j}b, \\ I_{j21} &= -\frac{1}{2}(\frac{1}{2}ab + y_{0j}a + x_{0j}b) - x_{0j}y_{0j}, \\ I_{j31} &= I_{j32} = 0, \\ I_{j22} &= x_{0j}^2 + \frac{1}{12}c^2 + \frac{1}{3}a^2 + x_{0j}a, \\ I_{j33} &= x_{0j}^2 + y_{0j}^2 + \frac{1}{3}(a^2 + b^2) + x_{0j}a + y_{0j}b, \end{aligned}$$

and the coupling matrix for rotational displacements of the main body and the displacements of element  $j$  can be written as follows:

$$W_j = \frac{\rho abc}{24} \begin{bmatrix} 0 & 0 & 0 & 0 & 0 & 0 & 0 & 0 & 0 & 0 & 0 & 0 \\ 0 & 0 & 0 & 0 & 0 & 0 & 0 & 0 & 0 & 0 & 0 & 0 \\ 6 & b & -a & 6 & -b & -a & 6 & -b & a & 6 & b & a \end{bmatrix} \quad (10)$$

### 3.0 PROBLEM IN FAST ATTITUDE MANEUVERS USING CONSTANT-AMPLITUDE INPUTS

In this study, it is supposed that the satellite has no control and no damping properties on the flexible solar panels. The control inputs for attitude maneuvers are only torques applied to the satellite's rigid main body, as results of on-off reaction jets of the thruster in constant amplitude. For such a system, the attitude angle acceleration of satellite as a rigid body motion can be written as

$$\begin{Bmatrix} \ddot{\phi} \\ \ddot{\theta} \\ \ddot{\psi} \end{Bmatrix} = \begin{bmatrix} I_{xx} & I_{xy} & I_{xz} \\ I_{xy} & I_{yy} & I_{yz} \\ I_{xz} & I_{yz} & I_{zz} \end{bmatrix}^{-1} \begin{Bmatrix} T_{bx} \\ T_{by} \\ T_{bz} \end{Bmatrix} \quad (11)$$

where  $I_{xx}$ ,  $I_{yy}$ ,  $I_{zz}$ ,  $I_{xy}$ ,  $I_{xz}$ , and  $I_{yz}$  are components of the inertia matrix  $\mathbf{I}$  of the whole satellite, and  $T_{bx}$ ,  $T_{by}$ , and  $T_{bz}$  are components of the torque input vector  $\mathbf{T}_b$  on the rigid main body. Integrating Eq. (11) with respect to time results the desired attitude angle velocity,

$$\begin{Bmatrix} \dot{\phi}_d \\ \dot{\theta}_d \\ \dot{\psi}_d \end{Bmatrix} = \int \begin{bmatrix} I_{xx} & I_{xy} & I_{xz} \\ I_{xy} & I_{yy} & I_{yz} \\ I_{xz} & I_{yz} & I_{zz} \end{bmatrix}^{-1} \begin{Bmatrix} T_{bx} \\ T_{by} \\ T_{bz} \end{Bmatrix} dt \quad (12)$$

and integrating once more gives a desired roll angle displacement,

$$\begin{Bmatrix} \phi_d \\ \theta_d \\ \psi_d \end{Bmatrix} = \iint \begin{bmatrix} I_{xx} & I_{xy} & I_{xz} \\ I_{xy} & I_{yy} & I_{yz} \\ I_{xz} & I_{yz} & I_{zz} \end{bmatrix}^{-1} \begin{Bmatrix} T_{bx} \\ T_{by} \\ T_{bz} \end{Bmatrix} dt dt \quad (13)$$

In the simulations, the main body of satellite is supposed to consist of six lumped masses at certain positions with respect to the satellite's center of mass. Values and positions of the lumped masses are listed in Table 1. Table 2 mentions parameters of satellite's flexible solar panels used in the computer simulations.

Table 1: Lumped masses consisting of the rigid main body

Mass (kg)	Position (m)		
	$x_b$	$y_b$	$z_b$
400	0.40	0.00	0.00
400	-0.40	0.00	0.00
500	0.00	0.50	0.00
500	0.00	-0.50	0.00
550	0.00	0.00	1.40
550	0.00	0.00	-1.40

Table 2: Parameters of the solar panels of satellite

Description	Values
Number of solar panels	2
Dimension of each solar panel (m <sup>3</sup> )	12 x 2.4 x 0.03
Young's modulus, $E$ (N/m <sup>2</sup> )	$0.6 \times 10^8$
Poisson ratio, $\nu$	0.3
Mass density, $\rho$ (kg/m <sup>3</sup> )	120
Number of elements in each solar panel	16
Dimension of each element, $b \times a \times c$ , m <sup>3</sup>	1.5 x 1.2 x 0.03
Offset angle, $\delta$ (degrees)	30
Distance between panel's root and $O_b$ , m	1.80

As the boundary condition for the model, the roots of solar panels are always in the straight lines. There are no deflections for the panel's roots from time to time. It means that  $\mathbf{d}_1$ ,  $\mathbf{d}_2$ ,  $\mathbf{d}_3$ ,  $\mathbf{d}_{28}$ ,  $\mathbf{d}_{29}$  and  $\mathbf{d}_{30}$ —those are components of  $\mathbf{d}$  in Eq. (5)—are all zero. Be noted that components of  $\mathbf{d}$  are measured in their respective local reference frames. This boundary condition is to represent the real fact that the roots of panels are usually strengthened using the bars or frames, those are relatively rigid, and then connected to the rigid main body using revolve joints.

For this configuration, the origin of the rigid main body fixed reference frame coincides with the centre of mass of the whole satellite in the undeform state,  $I_{xx} = 17,731 \text{ kg}\cdot\text{m}^2$ ,  $I_{yy} = 2,580 \text{ kg}\cdot\text{m}^2$ ,  $I_{zz} = 15,557 \text{ kg}\cdot\text{m}^2$ ,  $I_{xy} = I_{yz} = 0$ , and  $I_{xz} = 43 \text{ kg}\cdot\text{m}^2$ . At initial the satellite is at undeform condition, while the main body fixed frame and the orbital reference frame coincide with the inertial reference frame. The orbital frame,  $F_o$  rotates with respect to the inertial frame,  $F_i$  in constant angular velocity

$$\boldsymbol{\omega}_o = -\omega_o \mathbf{j}_i \quad (14)$$

where  $\mathbf{j}_i$  is the unit vector in  $Y_i$ -axis direction,  $\omega_o = 7.29 \times 10^{-5} \text{ rad/s}$ , so that  $F_o$  performs in  $F_i$  one rotation per sidereal day (24 hours of sidereal time or 23 hours 56 minutes 4.09054 seconds of mean solar time). The satellite is at rest condition with attitude angles of  $-3^\circ$  in roll,  $0^\circ$  in pitch and  $2^\circ$  in yaw at initial. The attitude will be maneuvered to the nominal operational attitude of geostationary satellite, i.e. roll, pitch and yaw angles are all  $0^\circ$ .

Then, it is supposed that the amplitude of torques in roll, pitch and yaw directions resulted by satellite's thruster are all 8 N-m. The shortest time duration torques of a series of alternating-sign constant-amplitude pulses to maneuver the satellite from one rest to other rest conditions is a bang-bang in maximum amplitude. The bang-bang input for these maneuvers will be two sequence pulses in the alternating sign in the same width. Under this limitation of torque, the profile of bang-bang torques needed consist of 21.528 seconds long of  $T_{bx}$  and 16.444 seconds long of  $T_{bz}$  bang-bangs. The satellite is subjected to the bang-bang roll and yaw torques simultaneously. Under these inputs, the roll and yaw angles change to the desired angular displacements, while pitch angle is not disturbed. After the torques were removed the roll and yaw angles still oscillate in large amplitudes. The dominant period for these oscillations is 18.7 seconds. This period is relating to the satellite's natural frequency resulted in calculation of 0.3354 rad/s. The total amplitude of residual oscillation is more than  $3.6^\circ$  for roll angle, as shown in Fig. 5(a), and more than  $1.4^\circ$  for yaw angle. The amplitudes of these residual attitude angle oscillations are greater than the desired attitude angle displacements. Such residual oscillations of course are very unacceptable for the precise-oriented satellite. As the attitude angles oscillate, the solar panels also vibrate. The largest residual

vibrations on solar panels happen at their tips. The node 25 experiences unlikely local vertical vibration with high deflection amplitude of 1.46 meters, as shown in Fig. 5(b). Compared with solar panel's length of 12 m, this deflection is about 12 %.

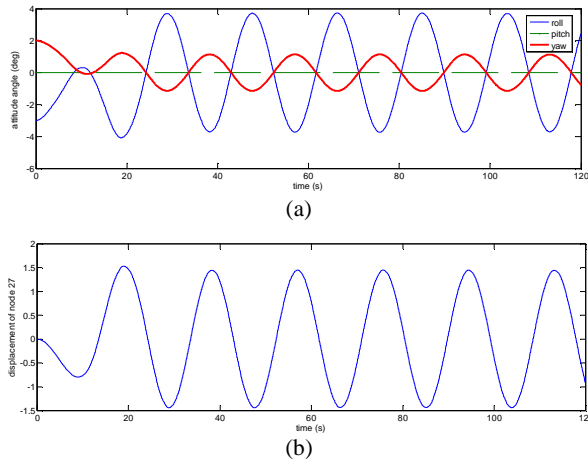


Figure 5: Time responses under the bang-bang and yaw torque inputs: (a) attitude angle displacement of the main body, (b) vertical displacement of node 27 of solar panel measured in local reference frame

#### 4.0 FUEL-EFFICIENT INPUT SHAPER FOR ATTITUDE MANEUVERS OF FLEXIBLE SATELLITE

A suitable torque input to maneuver the flexible satellite into the desired attitude angle with small or without residual vibration can be 'shaped'. The method is referred to as input shaping. In this method, amplitudes and time locations of the exciting input are determined by solving a set of constraint equations, for example:

- (a) constraints on the impulse amplitudes,
- (b) constraints on the rigid body motion,
- (c) residual vibration constraints, and
- (d) fuelling pulses duration.

The flexible satellite studied here is equipped with on-off reaction jets, so it cannot produce variable amplitude actuation thrust; the satellite must be maneuvered with constant amplitude torque pulses. For rest-to-rest maneuvers, the input must contain both positive and negative pulses so that the satellite can be accelerated and then decelerated back to zero velocity. If the number of impulse in shaping the input is selected as 8, the series of alternating-sign pulses for rest-to-rest fuel-efficient maneuver can be generated by convolving a step with an input shaper of the form [1]

$$\begin{bmatrix} A_i \\ t_i \end{bmatrix} = \begin{bmatrix} 1 & -1 & 1 & -1 & -1 & 1 & -1 & 1 \\ t_1 & t_2 & t_3 & t_4 & t_5 & t_6 & t_7 & t_8 \end{bmatrix} \quad (15)$$

In the fuel-efficient commands generated by equation (15), the fuelling periods happen at  $t_1-t_2$ ,  $t_3-t_4$ ,  $t_5-t_6$ , and  $t_7-t_8$ ; and the non-fuelling period at  $t_2-t_3$ ,  $t_4-t_5$ , and  $t_6-t_7$ . It means that the

command consists of two positive pulses and then is continued with two negative pulses. However, it is selected that the switching times from positive to negative pulses are at the same location, i.e.  $t_4 = t_5$  in this paper. Equation (15) becomes the first constraint, i.e. the constraint on impulse amplitudes. Equations (12)-(13) become the second constraints; in this study, the desired attitude angle velocity is  $\{0 \ 0 \ 0\}^T$  deg/s and the desired attitude angle displacement is  $\{3^\circ \ 0^\circ \ -2^\circ\}^T$ . The third constraint, the residual vibration at  $\omega = 0.3354$  rad/s, the natural frequency with strongest vibration, is set to be smaller than 0.01%,

$$V(\omega) = \sqrt{\frac{[\sum A_i \sin(\omega t_i)]^2 + [\sum A_i \cos(\omega t_i)]^2}{[\sum A_{bbj} \sin(\omega t_{bbj})]^2 + [\sum A_{bbj} \cos(\omega t_{bbj})]^2}} < 0.01\% \quad (16)$$

where  $A_{bbj}$  and  $t_{bbj}$  describe the input shaper corresponding to the bang-bang and are given by

$$\begin{bmatrix} A_{bbj} \\ t_{bbj} \end{bmatrix} = \begin{bmatrix} 1 & -2 & 1 \\ t_1 & t_2 & t_3 \end{bmatrix} \quad (17)$$

A lot of shaped inputs will be resulted by using the above three constraints. The fourth constraint is the length of pulses duration. Three cases are selected due to the pulses duration of the roll and yaw torque inputs. These three cases are listed in Table 3. In these selected inputs, each input has about similar duration length in fuelling pulses.

Table 3: Time location of impulses for shaping the torque inputs

	Pulses duration	$t_1$ (s)	$t_2$ (s)	$t_3$ (s)	$t_4$ (s)
Case 1	Roll, 1.2–1.3 s	0	1.204	46.834	48.074
	Yaw, 1.1–1.2 s	0	1.152	28.112	29.302
Case 2	Roll, 1.9–2.1 s	0	1.904	28.104	30.214
	Yaw, 2.7–2.8 s	0	2.782	9.372	12.152
Case 3	Roll, 4.2–4.3 s	0	4.284	9.364	13.584
	Yaw, 2.7–2.8 s	0	2.782	9.372	12.152

	$t_5$ (s)	$t_6$ (s)	$t_7$ (s)	$t_8$ (s)
Case 1	48.074	49.314	94.944	96.148
	29.302	30.492	57.452	58.604
Case 2	30.214	32.324	58.524	60.428
	12.152	14.932	21.522	24.304
Case 3	13.584	17.804	22.884	27.168
	12.152	14.932	21.522	24.304

#### 5.0 SIMULATION OF FLEXIBLE SATELLITE ATTITUDE MANEUVERS USING FUEL-EFFICIENT INPUT SHAPER

The simulation results of Cases 1, 2 and 3 are shown in Figs. 6, 7 and 8, respectively. We can see in Figs. 6(a), 7(a) and 8(a) that under the application of shaped inputs, the attitude angles of the satellite can be brought to zero degree successfully to all cases. The residual oscillation of attitude angle at  $\omega = 0.3354$  rad/s can be removed, but another oscillations at higher natural frequencies may occur. However, oscillation suppression at other frequencies is not designated in this paper. The paper focuses on the transient deflections of the flexible solar panels.

Case 1, where the lengths of pulses duration in roll and yaw

are input within 1.1 – 1.3 s, results 0.16 m maximum deflection of solar panel tip, i.e. node 27, during the maneuver process as shown in Fig. 6. This deflection is only 11% of the steady-state vibration amplitude after maneuver under the bang-bang torque inputs. Compared with solar panel's length of 12 m, this deflection is about 1.3%. In this case, the fuelling duration for roll is 4.888 s, while the fuelling duration for yaw is 4.684 s. Compared to the 21.528-s and 16.444-s lengths of roll and yaw fuelling durations of bang-bang inputs, respectively, these inputs consume fuel of 25.2% only. The attitude maneuver duration in this case is about 4.5 times of the bang-bang one.

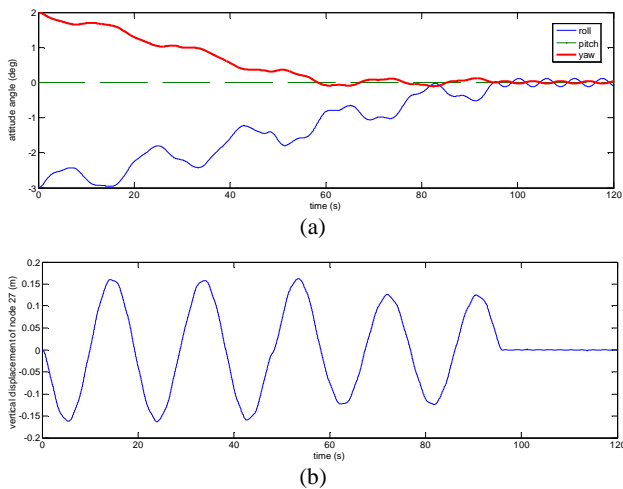


Figure 6: Time responses of Case 1: (a) attitude angle of the main body, and (b) local vertical displacement of node 27.

The application of 1.9 – 2.8 s lengths, or about twice of Case 1, of pulses duration in the torque inputs will result larger maximum deflection of node 27 during the transient response. We can see in Case 2 that the maximum deflection of the node 27 becomes 0.28 m at about  $t = 6$  s as shown in Fig. 7. This deflection is about 2.3% of the solar panel's length. In this case, the fuelling duration for roll is 8.028 s, while the fuelling duration for yaw is 11.124 s. The total length of fuelling durations of roll and yaw inputs is 50.4%, while the maneuver duration is about 1.6 times of the bang-bang ones.

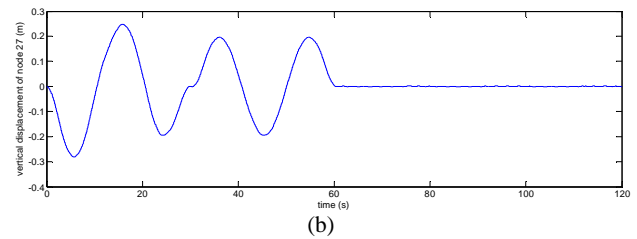
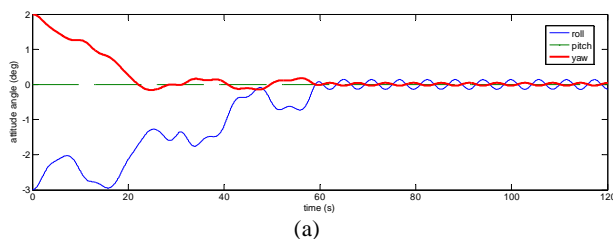


Figure 7: Time responses of Case 2; (a) attitude angle of the main body, and (b) local vertical displacement of node 27.

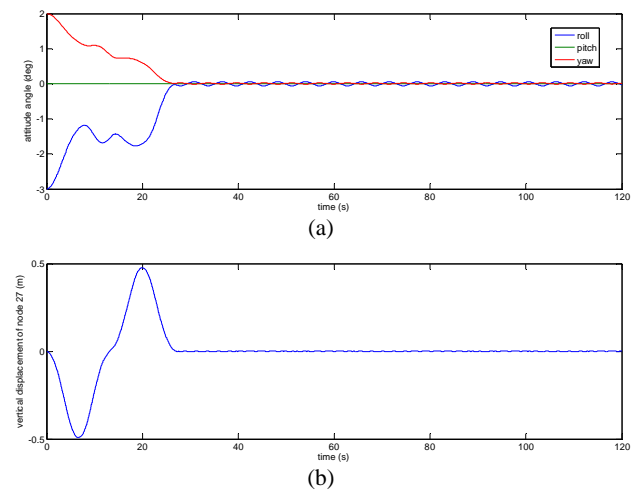


Figure 8: Time responses of Case 3: (a) attitude angle of the main body, and (b) local vertical displacement of node 27.

When the 2.7 – 4.3 s lengths of pulses duration, or about three times of those used in Case 1, are applied, the maximum deflection of node 27 during the transient response becomes larger than the resulted one in Case 2. We can see in Fig. 8 that the maximum deflection of the node 27 becomes 0.49 m, which happens at about  $t = 7$  s. This deflection is about 4.1% of the solar panel's length. The fuelling durations for roll and yaw are 17.008 s and 11.124 s, respectively. The maneuver duration is about 1.3 times, while the total length of roll and yaw fuelling durations is 74.1% of the bang-bang ones.

## 6.0 CONCLUSION

Attitude maneuver of the flexible satellite induces the vibration of flexible members as well as the main body oscillation. Using the bang-bang input, the flexible satellite has poor attitude accuracy after slew maneuver. For desired angle displacements of  $3^\circ$  in roll and  $2^\circ$  in yaw only, the satellite studied in this paper has  $3.7^\circ$  and  $1.3^\circ$  residual roll and yaw angle oscillations, respectively, and results 1.46-m amplitude of steady-state vibration of the tip of 12-m solar panel's length.

Shaped inputs show their capability to reduce steady-state oscillation and vibration after the maneuvers slightly. For the shaped inputs, eight impulses in fuel-efficient types are utilized here with the fourth and fifth impulses are at the same location.

For the maneuver duration less than 100 s simulated in the paper using about similar duration length of fuelling pulses, the maximum amplitudes of solar panel's tip deflection become smaller than 0.5 m. The longer the fuelling duration lengths in the inputs, the larger the maximum deflection of the tip during maneuver's transient response will be.

#### **ACKNOWLEDGEMENT**

The author would like to convey a great appreciation to Universiti Teknologi PETRONAS for supporting this research.

#### **REFERENCE**

1. Singhose, W., Bohlke, K. and Seering, W.P. (1995). *Fuel-efficient shaped command profiles for flexible satellite*, AIAA Guidance, Navigator, and Control Conference.
2. Parman, S. and Koguchi, H. (1998). *Rest-to-rest attitude maneuvers of a satellite with flexible solar panels by using input shapers*, Computer Assisted Mechanics and Engineering Sciences, Vol. 5 (4), pp: 421-441.
3. Parman, S. and Koguchi, H. (2000). *Fuel-efficient attitude maneuvers of flexible satellite with residual vibration reduction into an expected level*, Computer Assisted Mechanics and Engineering Sciences, Vol. 7 (1), pp: 11-21.
4. Parman, S. and Koguchi, H. (1999). *Controlling the attitude maneuvers of flexible satellite by using time-optimal/fuel-efficient shaped inputs*, Journal of Sound and Vibration, Vol. 221 (4), pp: 545-565.
5. Parman, S. and Koguchi, H. (1999). *Rest-to-Rest Attitude Maneuvers and Residual Vibration Reduction of a Finite Element Model of Flexible Satellite by Using Input Shaper*, Shock and Vibration, Vol. 6 (1), pp: 11-27.
6. Parman, S. (2013). *Controlling attitude maneuvers of flexible satellite based on nonlinear model using combined feedback-feedforward constant-amplitude inputs*, 10th IEEE International Conference on Control and Automation (ICCA).
7. Robertson, M.J. and Singhose, W.E. (2005). *Closed-Form Deflection-Limiting Commands*, American Control Conf., June 8-10 (Portland, OR, USA), Paper ThA11.3.
8. Robertson, M.J. (2008). *Transient Deflection Performance Measures for Command Shapers*, American Control Conf., June 11-13 (Seattle, Washington, USA), paper ThC10.1.
9. Bogner, F.K., Mallet, R.H., Minick, M.D. and Schmidt, L.A. (1965). *Development and evaluation of energy search methods of nonlinear structural analysis*, Flight Dynamics Lab. Report, AFFDL TR 65-113.